Preparation of Bio-Sensor with Nanofibers of Glucose Oxidase/Chitosan/Graphene Oxide for Detection of Glucose

Mahdizadeh, Bentolhoda; Maleknia, Laleh**+; Amirabadi, Amir
Department of Biomedical Engineering, South Tehran Branch, Islamic Azad University, Tehran I.R. IRAN

Shabani, Mohamad
Department of Biochemistry, Iran University of Medical Sciences, School of Medicine, Tehran I.R. IRAN

ABSTRACT: *In this paper, a Glassy Carbon Electrode (GCE) was modified with glucose oxidase (GOx)/chitosan (CS)/Graphene Oxide (GO) nanofibers for the detection of glucose via the electrospinning method. To do this, GOx was trapped among the two CS/GO nanofiber layers. Concerning electrochemical properties and producing conditions, the optimum amounts for GOx and GO in the deposited layer were 20 mg/mL and 20 % w/w, respectively. An investigation on the effects of pH, time of oxygen dissolving in the test solution, and scan rate on electrochemical behavior revealed that the peak current increased with increasing the oxygen dissolving time up to 20 min and scan rate values. However, the redox processes showed more symmetric anodic and cathodic structures at slow scan rates. Also, the highest current was obtained at a pH of 7.4. The result showed that the electrochemical process of GOx occurs through a two-proton and two-electron transformation. Additionally, the sensor exhibited excellent reproducibility and stability properties. It was concluded that the use of nanofibrous structure and the immobilization of the glucose oxidase among the two CS/GO nanofiber layers enhanced the electrochemical properties significantly due to the penetration of water-soluble glucose molecules in the porous nanofiber layers, which helped efficiently catalyze the oxidation of glucose and facile direct electron transfer for GOx. The resultant modified electrodes exhibited a high sensitivity of 1006.86 μA/mMcm^2 and a low detection limit of 0.02 mM with a wide linear range of 0.05–20 mM.*

KEYWORDS: *Graphene; Glucose Oxidase; Chitosan; Nanofibers; Cyclic voltammetry; Electrochemical biosensor.*

INTRODUCTION

Biosensors can be produced by combining molecular diagnostic elements with electrical or optical converters. Enzymes and antibodies can be considered as commonly used identification elements that are immobile at the surface of transducers [1-2]. Target molecules can be detected without adding additional reagents in these sensors.

* *To whom correspondence should be addressed.*
+E-mail address: malekniamood@yahoo.com
1021-9986/2022/12/3924-3938 15/$/6.05

Glucose is a concentrated element because of its vital effect in the treatment of diabetic patients. It plays a significant role in metabolism and disruption in glucose function due to insulin deficiency or resistance can lead to diabetes. Diabetes is a worldwide metabolic disease that affects millions of people throughout the world, and it is predicted that it will have reached up to half a billion by 2030 [3]. Diabetes causes minor vision loss, high blood pressure, heart disease, and kidney failure [4]. Glucose sensors are widely used in diagnostic tests to control diabetes in personal care, clinical laboratories, and hospitals. Recently, researchers have used nanomaterials to increase the performance of sensors [5].

Oxidoreductase is usually used to oxidize the glucose on the surface of the electrode when a glucose nanosensor is produced. Glucose oxidase (GOx) has been largely used for this purpose because of its high glucose selection, high stability, and high activity over a wide range of pH [6]. However, the structure, biological activity, and function of GOx change when they are applied directly to the naked electrode surface [7]. Efforts have been made to increase the GOx electron transfer at the electrode surface. To do this, the use of semiconductors, carbon materials such as carbon nanotubes, graphene, etc., and conductive polymers have been reported [8, 9]. For example, a glucose biosensor was developed based on the alginate-CuO and glucose oxidase (GOx) nano biocomposites films [10]. Glucose oxidase was stabilized on mesoporous carbon-ceramic materials, and its function as a biological sensor was studied [11]. Copper oxide nanocomposites/polypyrrole nanofibers/graphene oxide reduction was produced for glucose detection [12]. Glucose oxidase (GOx) was immobilized on a poly (p-phenylenediamine)/Fe_3O_4-modified glass carbon electrode to measure glucose [13].

Recently, graphene oxide has received much attention due to its unique nanostructure, high specific surface area, excellent optical, thermal, and mechanical properties, and small dimensions [14]. Also, large enclosed electrons provide a strong desire for carbon-based ring materials such as drugs, pollutants, and biomolecules. In addition, Graphene Oxide (GO) has unique electronic properties useful for making electrochemical sensors [15, 16]. Polyvinyl acetate electrode reinforced by MnO_2/CuO loaded on graphene oxide nanoparticles was produced as a glucose sensor [17]. Although GO plates are more hydrophilic than graphene, they are relatively hydrophobic, limiting their biological applications due to their extraordinary properties associated with single plates [18]. In this regard, the use of active surface and non-covalent adsorption of hydrophilic polymers on sheets was suggested by researchers [19]. Protected graphene was produced from polyvinyl pyrrolidone / ionic liquid electrochemical biosensor/GOx with the function of polyethylene to measure glucose [20]. Chitosan (CS), as a hydrophilic polysaccharide biopolymer, is the result of partial acetylation of chitin and has adhesion and non-toxic properties.

Moreover, chemical modifications are performed easily because of amino and hydroxyl groups in its structure [21]. Palladium/chitosan nanoparticles based on graphene were prepared as glucose biosensors [22]. A graphene/chitosan-modified electrode was fabricated for the selective detection of dopamine [23]. Cu nanoparticles deformed with gold-fiber nanoparticles have decorated graphene oxide particles as an electrochemical biosensor for glucose detection [4]. Also, a modified glucose oxidase-graphene-chitosan electrode was produced for direct electrochemistry and glucose measurement [24]. As mentioned above, chitosan, graphene oxide, and glucose oxidase were used in combination with various substances. However, a literary review showed that glucose was not detected by a glass electrode modified with chitosan/graphene oxide/glucose oxidase nanofibers. Nanofibers have unique properties due to their diameter between tens and hundreds of nanometers [25] and these future effects on the electrochemical properties of nanofiber-modified electrodes such as high surface area per unit volume, high porosity, and small interfacial pore size. In the present study, Graphene Oxide (GO)/Chitosan (CS) nanofibers were prepared to modify the surface of a Glassy Carbon Electrode (GCE). Glucose oxidase (GOx) was adsorbed on the surface of nanofibers as a catalyst. In order to maintain GOx at the nanofiber surface, another layer of CS/GO nanofibers was electrospun on the surface of the first layer. GOx was trapped between the two layers of CS/GO electrospun nanofibers. Also, the optimal values of GO and GOx in the modifier layer were determined according to the electrochemical properties and production conditions. The electrodes were described by various methods and analyzed by electrochemical tests.

EXPERIMENTAL SECTION

Materials

Chitosan (CS) (molecular weight: 45 kDa and degree of acetylation> 75%) and glucose oxidase (GOx) (EC 1.1.3.4, Type X-S, 40,300 U/g) are provided by Aldridge, Germany. Graphene oxide (GO) nanoparticles (99%, 4-7 nm, and 1-6 layers) were purchased from US Research Nanomaterials. Acetic acid (98%) and monopotassium phosphate (KH_2PO_4), and dipotassium phosphate (K_2HPO_4) salts were prepared by Merck.

Preparation of chitosan/graphene oxide (CS/GO) composite nanofibers

The electrospinning solution was prepared by dissolving 0.15 g of chitosan in 10 mL of acetic acid. The mixture was sterilized at 65 ℃ for 12 h to obtain a homogeneous chitosan solution. Then, different amounts of GO (0.5, 1, 1.5, 2, 2.5, and 3 wt%) were added to the chitosan solution, and the mixture was placed in an ultrasonic machine for complete dispersion of the CS/GO solution. The prepared solutions are poured into plastic syringes, and the electrospinning process is performed under voltage; the distance between the needle tip, the collector, and the injection rate is 20 kV, 12 cm, and 0.5 mL/h, respectively. The electrospinning device is from Nanoscale Technologists Company (Iran), and the nanofibers are collected on aluminum paper.

Preparation of modified GCE with nanofibers (CS/GO) and encapsulated glucose (GOx)

First, GCE is polished with alumina powder (0.3 and 0.05 microns) and then washed and dried with distilled water. In order to correct GCE with CS/GO/GOx electrospinning solution, CS/GO solution was electrified on GCE surface, and then 0.1 µl of GOx solution (with different concentrations of 5, 10, 20, and 30 mg/mL) was dripped on the surface of nanofibers. After the solution dries at 4° C, the new electrospinning layer is placed on the surface of the first layer with the previous conditions.

Materials characterization

The surface morphology of the nanofibers was investigated using a field scanning electron microscope (FESEM). This analysis was performed with the TE-SCAN MIRA3 device. The constituents of the nanofibers were also determined by X-ray energy-dispersing microanalyzer (EDS, Oxford Instruments, UK). Different nanofibers were also tested by Fourier Transform InfraRed (FT-IR) (Bruker Tensor 27, Equinox 55). The surface area of the nanofibers was measured using a Brunaur-Emmett-Teller analyzer (BElSORP Mini from Microtrac Bel Corp). The pore size distribution was calculated using a Barrett-Joyner-Halenda analyzer based on the nitrogen desorption isotherm by source porosity. This test was also performed by the BElSORP Mini device from Microtrac Bel Corp. Surface topography of different nanofibers was performed using an atomic absorption microscope (ENTEGRA MDT-AFMNT device of NT-MDT company). The structure of nanofibers and the presence of graphene oxide were confirmed by Transmission Electron Microscopy (TEM) (PHILIPS CM30, NETHERLANDS) at an acceleration voltage of 200 kV. The thickness of the samples was measured using a CH-1S thickness gauge.

Electrochemical studies

Cyclic Voltammetry (CV) has been performed using an electrochemical device (potentiosta/galvanosta) (model PGSTAT100 from Metrohm, UK) with three electrodes with modified or carbonized glass electrode (GCE, d= 3mm) as the working electrode. A platinum wire and Ag/AgCl (saturated KCl) were used as the counter and reference electrodes, respectively. The experiments were performed in buffer solution (0.1 M) without glucose and in the presence of glucose with different concentrations (0-100 mM). The effect of pH (4-8), oxygenation time (5-30 minutes), and GOx concentration on electrochemical properties have also been investigated. The flow of oxygen is maintained in the solution during the electrochemical process. The surface area of the prepared electrode is 2.8 per square centimeter.

RESULTS AND DISCUSSION

Characterization

FESEM images of chitosan and CS/GO nanofibers with different percentages of GO are shown in Figure 1. As can be seen, chitosan nanofibers have a uniform morphology with a smooth surface. For CS/GO nanofibers, a uniform, moth-free morphology has been observed when containing GO in the range of 0.5-2% by weight, which may result from the proper dispersion of GO nanoparticles in the polymer matrix. It has already been stated that chitosan and graphene oxide can form a good mixture and homogeneous solution, and the resulting mixture is stable at room temperature [26].

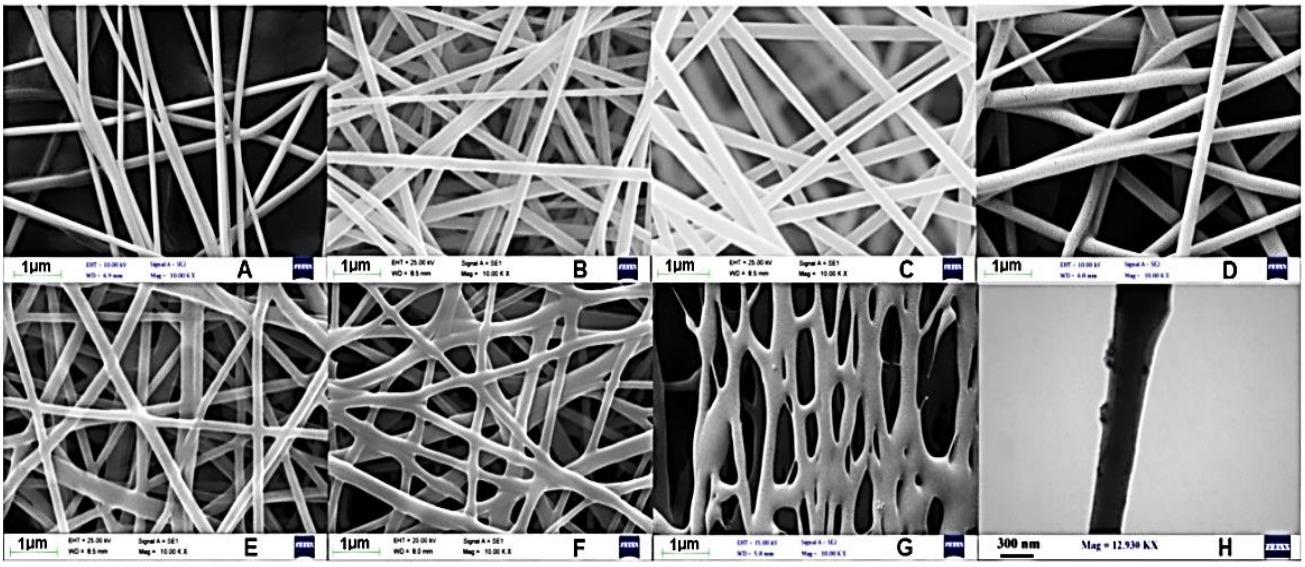

Fig. 1: FESEM nanofiber images: (A) CS (B) CS/GO/0.5, (C) CS/GO/1, (D) CS/GO/1.5, (E) CS/GO/2, (F) CS/GO/2.5, CS/GO/3 (G) and (H) TEM image of CS/GO/2 nanofibers.

However, as GO concentration in nanofibers increases, the uniformity declines. Also, some adhesions have been seen, especially at the junctions of nanofibers. According to the images, the morphology of nanofibers changes when the amount of GO is increased to 3% by weight, which depends on the amount of crosslinking between the polymer chains, which increases the viscosity of the spinning solution. It has been reported that the higher adhesion of polymer chains is due to the higher viscosity [27].

The diameter distribution diagram of nanofibers for different samples is shown in Figure 2. As can be seen, the addition of GO to the chitosan polymer increased the diameter of the nanofibers. Mean nanofiber diameters for CS, CS/GO/0.5, CS/GO/1, CS/GO/1.5, CS/GO/2, CS/GO/2.5 and CS/GO/3 respectively 11/105, 37/121, It is 159.59, 188.45, 261/97, 326.38 and 386.49 nanometers. The resulting nanofiber diameter distribution confirms the formation of crosslinks among polymer chains. Similar results have been reported by other researchers [28]. From FESEM images, it can be seen that 2% by weight of GO is the optimal amount. The TEM image of CS/GO/2 nanofibers is shown in Figure H1. The presence of GO on the surface of nanofibers is marked as dark spots.

Microscopic images of samples containing different amounts of GOx are shown in Figure 3. As shown in the pictures, after adding GOx, a layer is placed on the surface of the nanofibers. The layer thickness increases as the GOx values increase to 10 and 20 mg/mL. For CS/GO/2/GOx/20, some cracks and pores have been observed on the surface of the nanofibers, possibly due to the interaction of GO, the CS, and GOx chains. Increasing the amount of GOx to 30 mg/mL causes the pores to fill between the nanofibers, and the morphology of the nanofiber layer changes from nanofiber to film. The average diameters of nanofibers are CS/GO/2/GOx/5, CS/GO/2/GOx/10 and CS/GO/2/GOx/20, respectively, 270.55, 280.5 and 291.5 nm. The TEM image of CS/GO/2/GOx/20 nanofibers is shown in Figure D3, which shows the shell-brain structure of the nanofibers. According to the figure, a thin layer thickness of 21 nm is placed on the surface. Therefore, it can be concluded that 20 mg/mL GOx is the optimal amount.

AFM analysis can be a good way to check for the presence of nanoparticles on the surface of nanofibers. The various AFM images of CS, CS/GO/2, CS/GO/2/GOx/20, and CS/GO/2/GOx/30 nanofibers are shown in Figure 4. Mean surface roughness (Sa) of the roughness profile for CS, CS/GO/2, CS/GO/2/GOx/20 and CS/GO/2/GOx/30 samples respectively 20.2, 29.7, 1.29 and 27.3 nm is calculated. It is observed that the amount of Sa increased after the addition of GO to the polymer matrix, which is related to the accumulation of nanoparticles in nanofibers [29]. In previous research, it has been reported that graphene sheets in composites are crumpled and wrinkled [30]. The value of Sa for the CS/GO/2/GOx/20 sample is significantly reduced compared to the CS/GO/2 sample, which can be due to the presence of

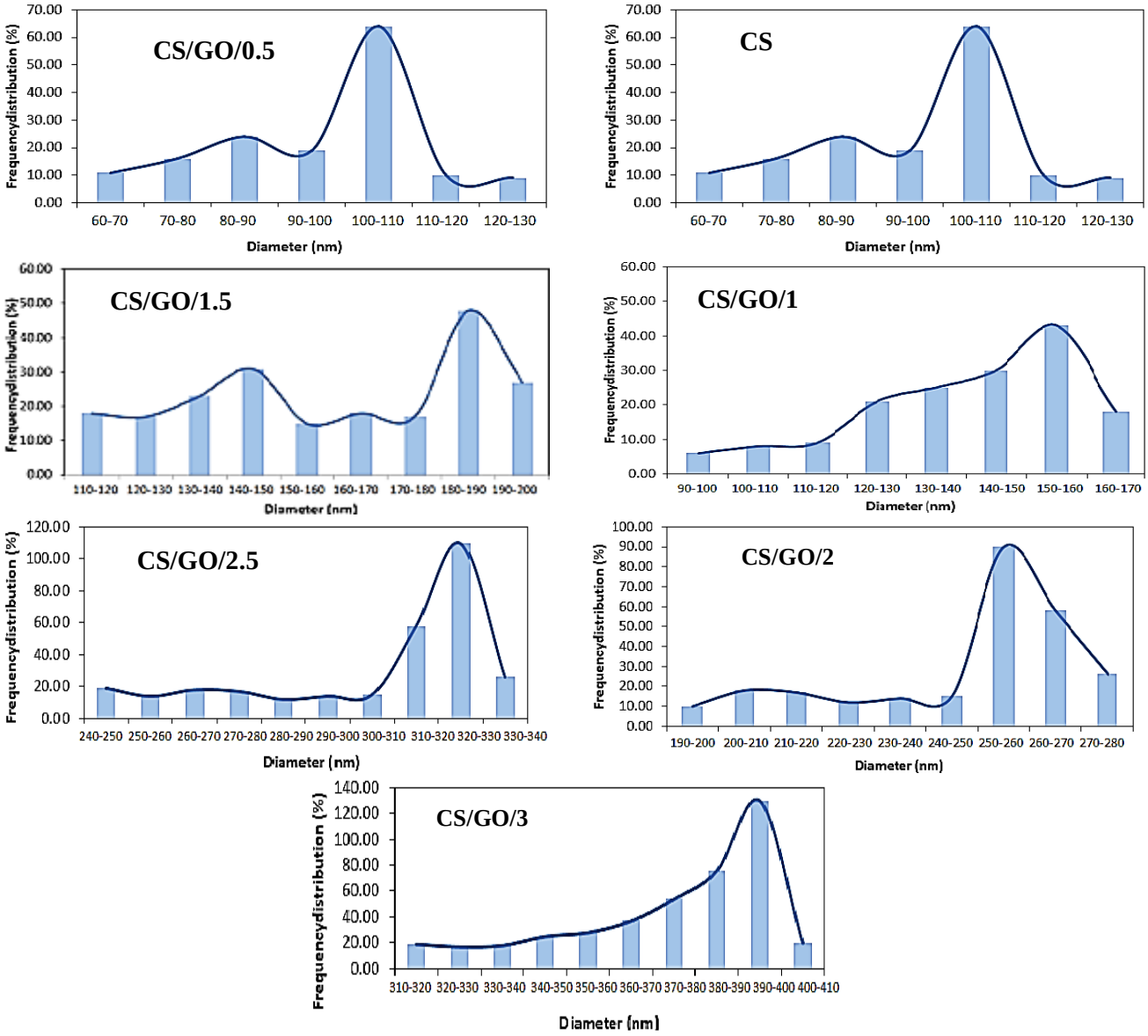

Fig. 2: Diagram of nanofiber diameter size distribution for different samples.

GOx on the surface of nanofibers, which increases the adhesion of nanofibers and fills the cracks on the surface of CS/nanofiber. The value of Sa for CS/GO/2/GOx/30 is the lowest among the samples due to the change in the morphology of the sample from nanofiber to film.

The FT-IR spectra of CS/GO/2 and CS/GO/2/GOx/20 nanofibers are shown in Figure 5. For CS/GO/2, the 3418 1/cm band corresponds to the overlap of the NH tensile vibration in CS and the tensile vibration of the OH bands in GO. Also, the band at 1684 1/cm is related to the vibrations of the COOH group in GO, which are transmitted to lower wavelengths (the tensile vibration of the COOH group in pure GO appears at 1719 1/cm [31]). The peak at 1608 1/cm corresponds to the C = C groups of graphene oxide, which are transmitted at lower wavelengths compared to the pure GO that appears at 1630 1/cm [32]. These observations are due to the formation of hydrogen bonds between GO and the chitosan hexa ring. The peak observed in 1571 1/cm is related to the vibration band of the chitosan secondary amine group [33]. C-OH and C-O-C vibration peaks in GO layers were observed in 1383 1/cm and 1071 1/cm, respectively.

For nanofibers, CS/GO/2/GOx/20, 1/cm band 1544 and 1640 1/cm are related to the flexural vibration of NH amide (II)

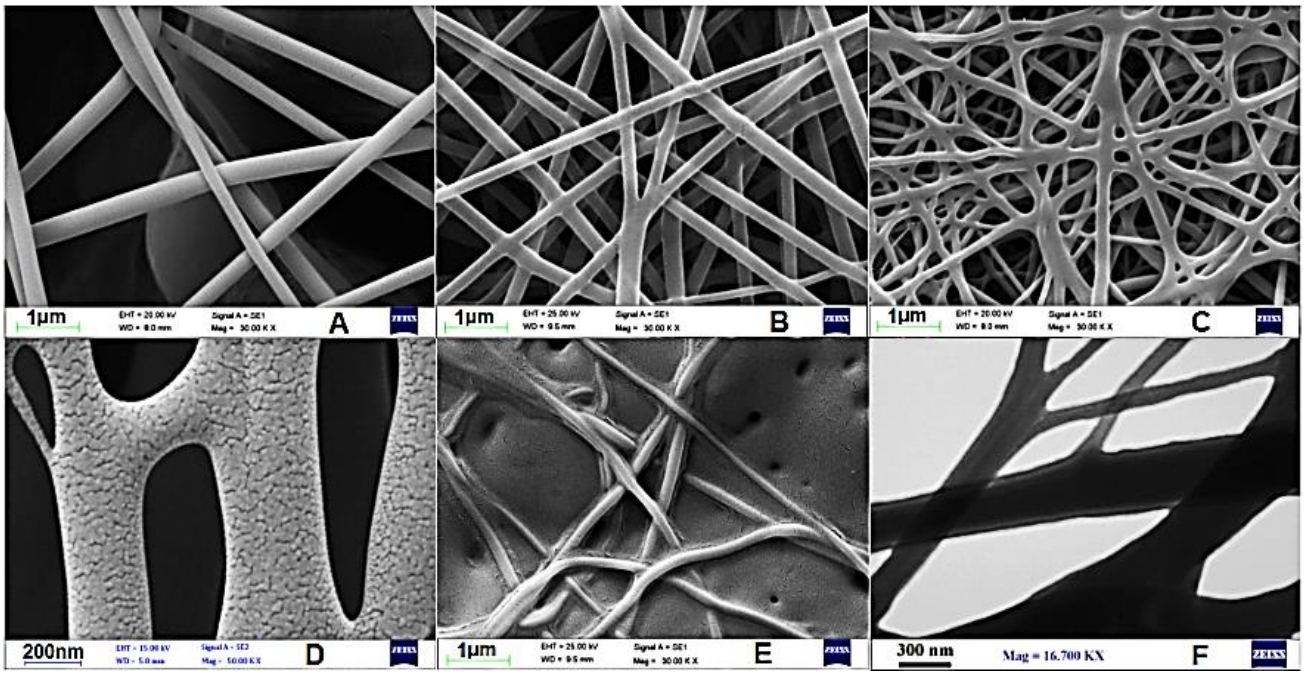

Fig. 3: FESEM images of nanofibers: (A) CS/GO/2/GOx/5 (B) CS/GO/2/GOx/10, (C, D) CS/GO/2/GOx/20, (E) CS/GO/2/GOx/30, (F) TEM image of CS/GO/2/GOx/20 nanofibers.

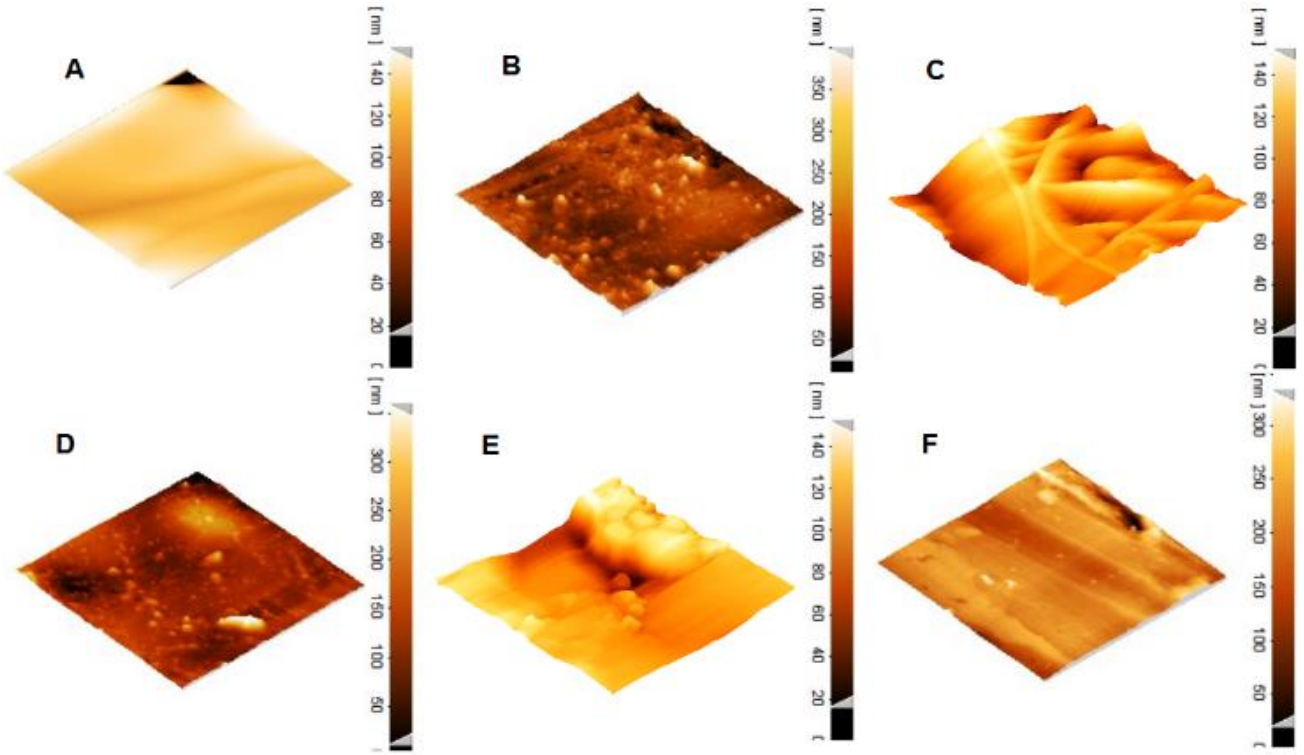

Fig. 4. AFM images of nanofibers: (A) CS (B, C) CS / GO, (D, E) CS / GO / 2 / GOx / 20, (F) CS / GO / 2 / GOx / 30.

and the tensile vibration of C = O amide (I) group. The peak 1077 1/cm is related to the tensile vibrations R-C=O (steel group) or C-O (alkoxy group). The wavelengths of this peak show a decrease compared to pure GO reported at 1100 1/cm [34] and indicate the formation of hydrogen bonds between GOx and GO. 3298 1/cm bond is related

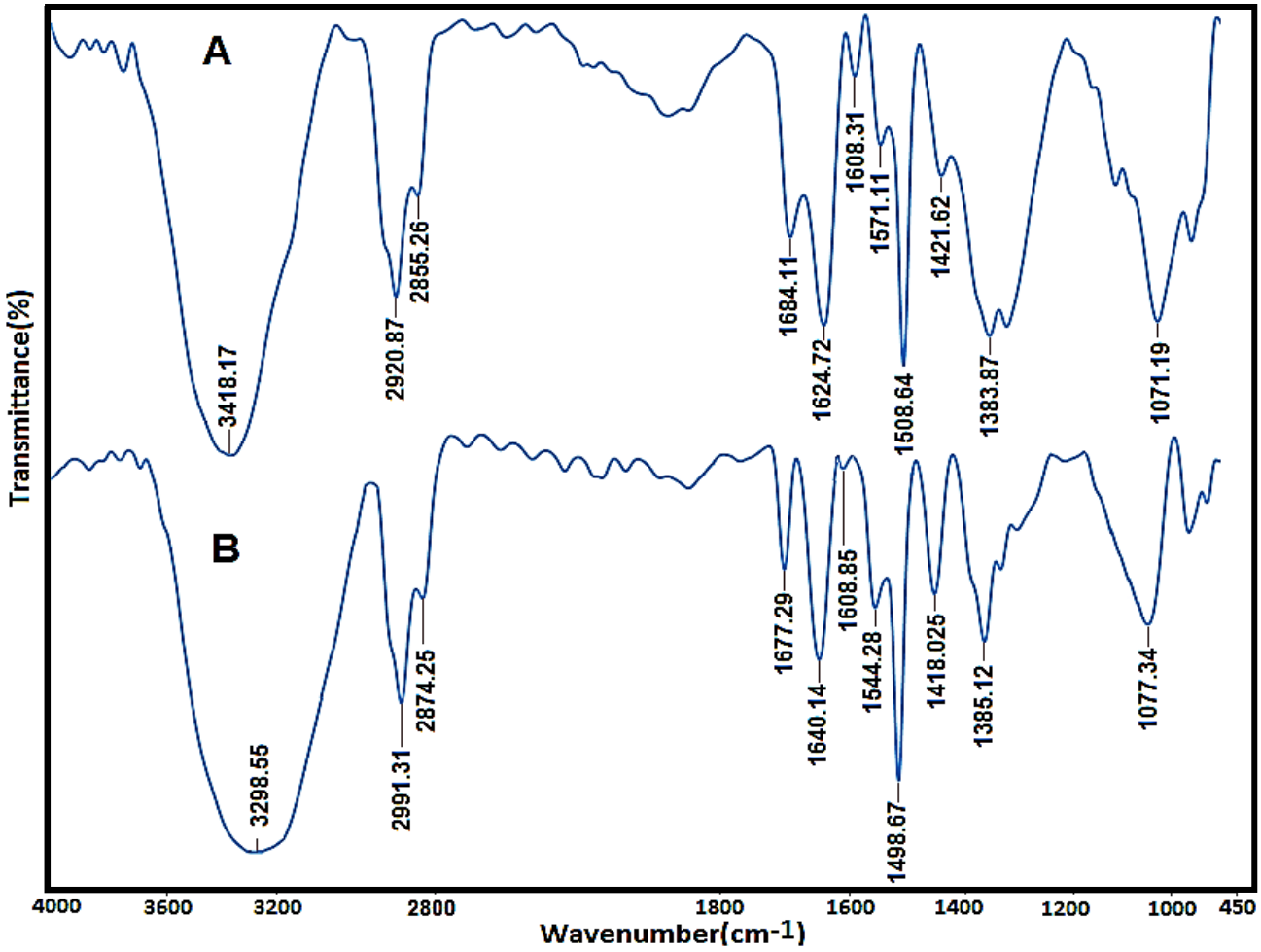

Fig. 5: FT-IR nanofiber images: (A) CS/GO/2 (B) CS/GO/2/GOx/20.

the overlap of tensile vibrations of OH and NH groups. As can be seen, the peak is wider and transmitted to lower wavelengths, which confirms the formation of hydrogen bonds between GOx and GO relative to CS/GO. The other observed peaks are similar to the CS/GO spectrum.

BET and BJH analyses were performed to confirm that the selected values are optimal for GO and GOx. BET values for different samples are given in Table 1. As can be seen, the BET value for CS nanofibers is 233.37 m^2/kg, which has increased to 240.05 and 361.65 m^2/kg for CS/GO/0.5 and CS/GO/2, respectively, due to the addition of GO with the surface area is high to chitosan polymer. As the amount of GO increases to 2.5% and 3% by weight in composite nanofibers, the amount of BET decreases, which can be related to the accumulation of nanoparticles and the adhesion of nanofibers. The results of FESEM and BET analyses show that 2% by weight of GO is optimal. The BET value for nanofibers is CS/GO/2/GOx with different amounts of glucose oxidation. It is clear that increasing the amount of GOx to 20 mg/mL leads to an increase in the amount of BET, which is probably due to the formation of a hole in the sample. The cause of this phenomenon is not known to us, but it could probably be due to the interaction of CS, GO, and GOx with each other. The presence of pores on the surface of CS/GO/2/GOx/10 and CS/GO/2/GOx/20 nanofibers is confirmed by the pore size distribution curves (Figure 6). As shown in Figure 6, relatively narrow rod structures with centers of 490, 576, 689.5, 710, 835.3, and 488.1 nm for CS, CS/GO/2, CS/GO/2/GOx/5, CS, respectively. GO/2/GOx/10, CS/GO/2/GOx/20 and CS/GO/2/GOx/30 have been observed. For CS/GO/2/GOx/10 and CS/GO/2/GOx/20 nanofibers, peaks at 21 and 26.4 nm have been observed, indicating the mesoporous structure of the nanofibers [38]. Increasing the pore volume values is related to increasing the average diameter of nanofibers [39, 40].

Table 1. BET values of different samples.

Sample	BET (m^2/g)	Vm (cm^3/g)	Vm (cm^3/g)	BET (m^2/g)	sample
CS	233.37	25.97	36.64	350.14	CS/GO/2/GOx/5
CS/GO/0.5	240.05	26.98	33.98	363.52	CS/GO/2/GOx/10
CS/GO/1	268.41	29.17	40.31	376.44	CS/GO/2/GOx/20
CS/GO/1.5	311	33.68	23.35	101.77	CS/GO/2/GOx/30
CS/GO/2	361.65	38.1			
CS/GO/2.5	315.35	34.04			
CS/GO/3	277.16	29.85			

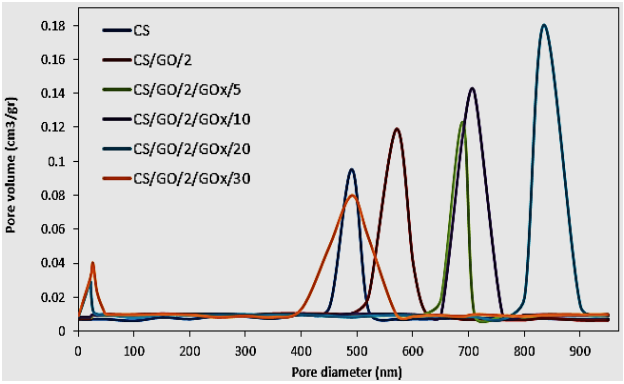

Fig. 6: Pore size distribution curves of different samples.

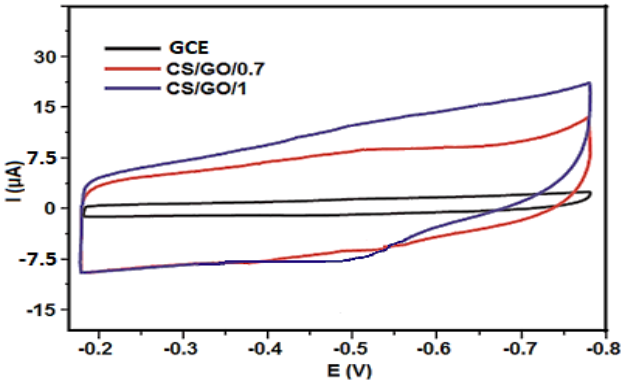

Fig. 7: Comparison of cyclic voltammetry of GCE electrode and GCE-CS/GO/0.7 and GCE-CS/GO/1 electrodes (10 mV/g, GO concentration equal to 2 wt%, phosphate buffer 0.1 M and 7.4 = pH)

Electrochemical studies

Investigate the relationship between electrospun layer thickness and electrochemical properties

In order to investigate the relationship between the thickness of the electrospun layer and the electrochemical properties, two different amounts of electrospinning solution (0.7 and 1 mL) were electrified on the surface of the GCE electrode. Experiments were performed on a 0.1 M oxygen-saturated phosphate buffer (pH = 7.4) without glucose at a scan rate of 10 mV/s. The thickness of the layer for solution for injection was 0.7, and 1 mL was 389.7 and 645.3 µm, respectively. Figure 7 shows the CV curve for GCE and CS / GO with different thicknesses.

As can be seen, the current is increased by increasing the amount of polymer injection (layer thickness), which is related to improving the electrical conductivity by increasing the amount of GO with high conductivity in the electrified layer and rapid electron transfer. However, the difference between the cathode peak current for the electrode with 0.7 and 1 mL of polymer values is not significant. On the other hand, electrode production time can be an essential parameter in new electrode production. For this purpose, 0.7 mL of injected polymer is selected as the optimal.

Investigation of the effect of GOx

The effect of GOx value on electrochemical properties has been investigated by different values of GOx on the electrode surface, and the results are shown in Figure 8. As shown in the figure, the amount of GOx in the nanofiber layer increases the flow. Also, the redox peak voltage is transferred to higher values. The biocatalytic reaction of glucose oxidation is performed by reducing the flavin group of the enzyme by the glucose reaction. This reaction continues with re-oxidation of flavin by oxygen and reduction of the oxidized form of flavin [41-42]. Glucose biosensors based on direct electrochemical behavior between the electrode and trapped glucose oxidase have been highly recommended due to their high selectivity, sensitive glucose detection, and relatively low manufacturing cost [43, 44]. Figures 7 and 8 show that no peak is observed in the voltammetric curve of the GCE-CS / GO cycles, but a separate redox peak pair is obtained at the electrode containing GOx, indicating the GOx redox peak. The maximum anodic potential peak (Epa) and the maximum cathodic potential peak (Epc) is observed at -0.473 and -0.529 volts, respectively. Also, the maximum

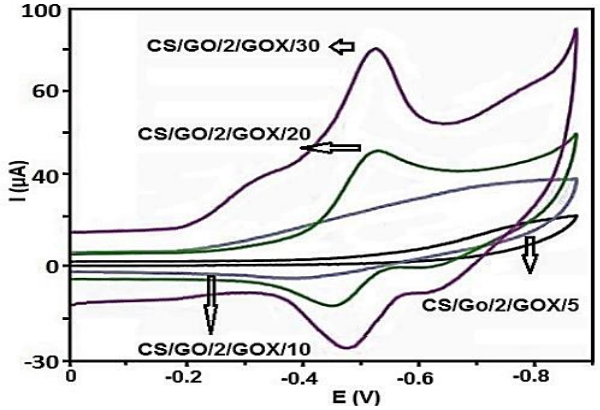

Fig. 8: Modified GCE cycle voltammetry with different amounts of GOx in oxygen-saturated phosphate buffer at a scan rate of 10 mV/s and a glucose concentration of 0.1 mM.

peaks of anodic and cathodic currents (Ipa and Ipc) are observed at 43.9 and -15.8 microamperes, respectively.

It is clear from the results that the current and potential of CS/GO/GOx nanofibers are higher than similarly modified electrodes [45, 46], and it is related to the high surface area and porous structure of nanofibers that increase the interaction between GOx, GO and the electrode. However, the flow and potential values for CS/GO/2/GOx/30 are very close to the sample values of CS/GO/2/GOx/20, which could be due to the filling of the pores in the nanofibers. It can reduce the porosity and surface area of the nanofiber layer and limit the interaction of GOx, GO, and GCE. Therefore, 20 mg/mL is the optimal amount selected. The results of BET and BJH analysis are in complete agreement with the results othe f electrochemical analysis.

Investigate the effect of scanning speed

The results of the effect of different scan speeds on electrochemical properties are shown in Figure A9. As shown in the figure, as the scan speed increases from 10 to 100 mV/s , the redox current also increases, indicating a GOx redox reaction on the electrode surface, which is a quasi-reversible controlled electrochemical process [47]. However, the redox process shows more anodic and cathodic structures at low scan speeds.

Linear diagrams of anode and cathode current versus scan speed are shown in Figure B10. As can be seen, as the scan speed increases, the redox peak current increases linearly. The GOx surface coverage is calculated according to Equation (1) using the slope value of the scan speed and peak flow diagrams [48].

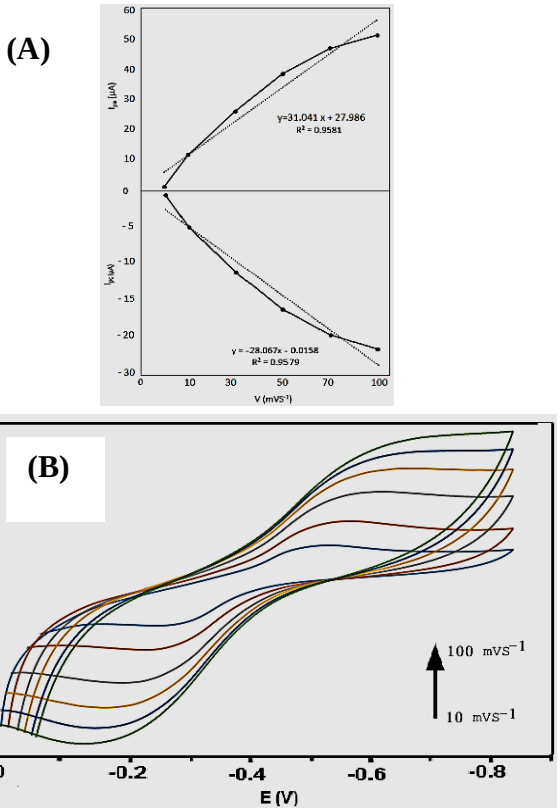

Fig. 9: A) Cyclic voltammetry of CS/GO/2/GOx/20 in phosphate buffer with different scan speeds of 10, 30, 60, 100, 120, and 150 B) Linear diagram of peak current versus scan speeds.

$$Ip = \frac{n^2F^2vAD}{4RT} \quad (1)$$

Where Ip, n, A, F, D, V, R, and T are the maximum current in the impedance, the number of electron transitions in the redox process, the electrode area in square centimeters, the Faraday constant in Kelvin per moles, the surface coverage in terms of moles per square centimeter, and concentration in terms of moles per square centimeter, scan speed in volts per second, gas constant in joules in terms of kelvin per moles, and temperature in terms of kelvins. Assuming the number of electrons transferred in the redox is equal to 2 (n= 2), the value of the parameter D is set at 1.8 x 10.4 mol per square centimeter. The presence of more active sites on the surface of nanofibers is the reason for the appearance of more D values [49]. According to the value of R2, the curves (Figure B10) have linear relations. Also, the peak-to-peak separation is small, which confirms that the modified electrode redox process is a reversible and surface-limiting process. The potential difference (ΔEp) can be calculated by Equation (2), and then the electron transfer rate can be determined.

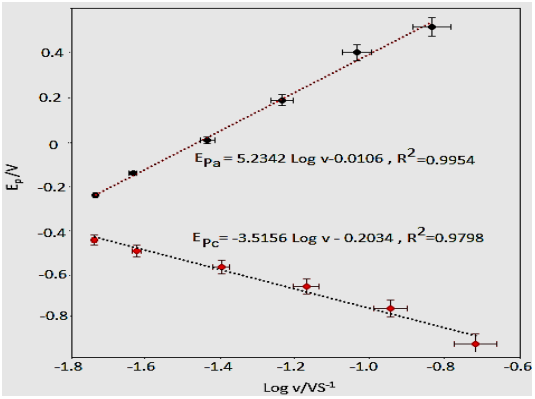

Figure 10. Diagram of peak potential (Ep) versus the logarithm of scan speed at different scan speeds from 10 to 150 mV /s.

$$\Delta E_P = |E_{PC} - E_{Pa}| \quad (2)$$

Where Epa and Epc are the anodic and cathode voltages, respectively.

The Epa and Epc diagrams versus the logarithm of the scanning speeds are shown in Fig. 11.

The transfer rate constant (ks) for GOx in the modified GCE can be estimated using the Lawrence model (Equation (3)) [50].

$$\log Ks = \propto \log(1-\propto) + (1-\propto)\log \propto - \log\frac{RT}{nFv} - \frac{\propto(1-\propto)nF\Delta Ep}{2.3RT} \quad (3)$$

Which *ks* is the transfer coefficient, *n* is the number of electrons transferred, and α is the standard heterogeneous velocity constant, *V* is the displacement velocity (volts per second), *R* is the gas constant (joules per Kelvin in moles), *F* is the Faraday constant, and *Ep* is the cathodic peak potential. Using the slope of the curves in Figure 10, α is calculated to be 0.49. Also, the ks value for the modified GCE is set at 3.27 per second. The electron transfer rate indicates the rate of reduction of the oxidation reaction on the electrode. The value of ks further improves the communication between the active GOx site and the electrode.

Investigate the effect of pH

The effect of solution pH on the electrochemical behavior of the prepared electrode was investigated, and the results are shown in Figure 11. According to the figure, it can be seen that increasing the pH value has transferred the anodic and cathodic potential to lower values, and this is due to the FAD redox process, in which both anodic and cathodic peak currents have increased. The maximum current was obtained at pH = 7.4, and a further increase

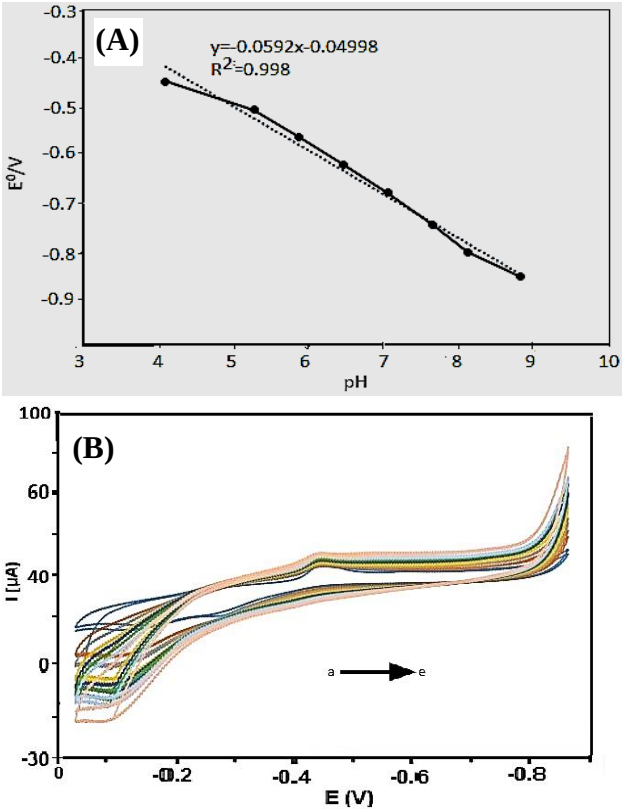

Fig. 11: A) The voltammetry of the electrode cycles prepared in the phosphate buffer solution with different pH values (ae) equal to 6.5, 7.4, 8.2, 9, and 9.5 with a scan speed of 10 mV/s B) Linear diagram of potential Redox versus pH.

in pH decreased the amount of current, which could be due to the degradation of the enzyme and H + rEquired compounds for the electrochemical process. Previous research has also reported that the biological activity of GCE-modified GCE is pH-dependent. The relationship between pH and redox potential (E'0) is shown in Figure B11. It can be seen that the redox potential has changed linearly in the pH range of 3.5-9.5 with a slope of -5.25 mV on pH. This value is close to the theoretical value of -58.6 millivolts per pH, which indicates the transfer of two protons and two electrons in the electrochemical process [51].

Glucose diagnostic test

Glucose detection was performed by changing the glucose concentration in the electrochemical test solution, and the results are shown in Figure 12. After adding glucose, the cyclic voltammetric shape changed with increasing peak reaction current and decreasing oxidation. The addition of an electrocatalytic reaction (Equations (7) and (8)) is inhibited by reducing the concentration of the oxidized form of GOx

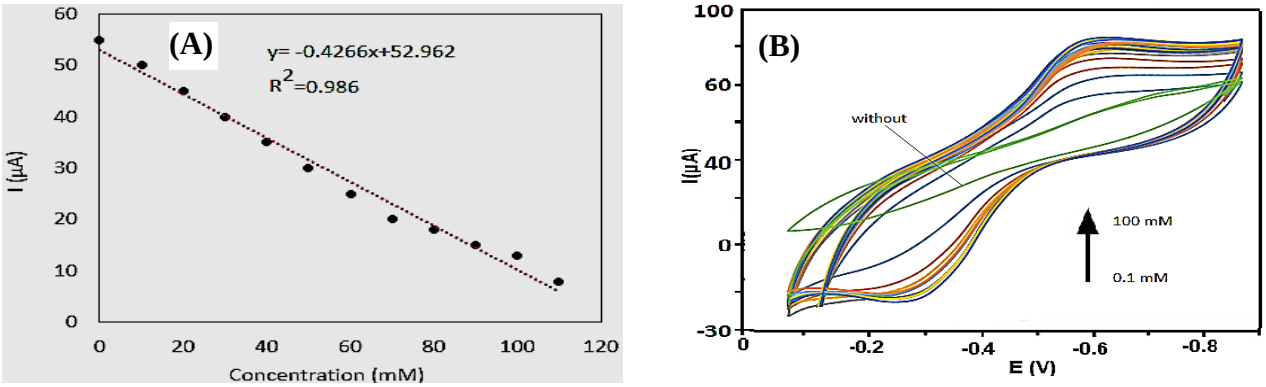

Fig. 12: A) Voltmetry of the modified electrode cycle in an oxygen-saturated phosphate buffer solution (0.1 M, pH= 7.4) at different glucose concentrations and a scan rate of 10 mV/s, B) Calibration curve: Linear correlation between currents Cathodic peak with glucose concentration.

on the electrode surface by a catalytic-enzyme reaction (Equation (9)) and reduces the reaction current.

The cathodic peak current (Ipc) is related to the GOx reaction (FAD). However, the peak anodic current (Ipa) is related to the oxidation (FADH2) of GOx [51]. Reduction in flow is also related to oxygen consumption [52].

$$GOD(FAD) + 2H^+ + 2\,e^- \leftrightarrow GOD\,(FADH_2) \quad (7)$$

$$GOD(FADH_2) + O_2 \rightarrow GOD\,(FAD) + H_2O_2 \quad (8)$$

$$GOD\,(FAD) + glucose \rightarrow GOD\,(FADH_2) + gluconolactone \quad (9)$$

The calibration curve shows a linear region of cyclic voltammetric current versus glucose concentration in Figure B12. Depending on the shape, the linear region is in the concentration range of 0.05 to 20 mmol. Also, the sensitivity and detection were 6.86 µA/mm and 0.02 µM, respectively [52-54].

Numerous articles have suggested that biosensors may be a good choice for determining human blood glucose levels. It has also been reported that the normal range of blood glucose concentrations is 4.6-6.6 mM, and concentrations above 7 mM are considered as diabetic levels [54].

Electrocatalytic behavior of the modified electrode with respect to oxygen

The mechanism for detecting glucose with GOx is based on the detection of H_2O_2, which is produced during glucose oxidation in the presence of dissolved oxygen. The glucose detection mechanism is presented in Equations (11) and (12).

The reason for electron transfer between GOx and the electrode is the rapid conversion of (FAD) GOx to ($FADH_2$) GOx. Then, ($FADH_2$) GOx electrocatalizes

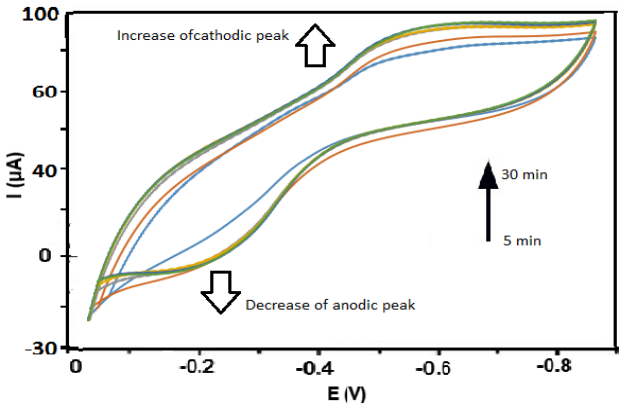

Fig. 13: Voltmetry of the modified electrode cycle in phosphate buffer solution (0.1 M, pH= 7.4) at a concentration of 0.1 mM glucose and different oxygenation times of 5, 10, 15, 20, 25 and 30 minutes.

dissolved oxygen by reproducing (FAD) GOx (Equation (13)); These reactions are repeated many times.

$$Glucose + O_2 \rightarrow Gloconolactone + H_2O_2 \quad (10)$$

$$GOD(FAD) + 2H^+ + 2\,e^- \rightarrow\leftrightarrow GOD\,(FADH_2) \quad (11)$$

$$H_2O_2 \rightarrow O_2 + 2\,e^- + 2H^+ \quad (12)$$

$$GOD(FADH_2) + O_2 \rightarrow GOD\,(FAD) + H_2O_2 \quad (13)$$

The H_2O_2 produced is oxidized by an electrochemical reaction to produce a redox current, proportional to the glucose concentration in the test solution. The effect of dissolved oxygen in solution on electrochemical properties has been investigated by different times of the presence of dissolved oxygen (5-30 minutes). The results (Figure 13) show an increase in peak current with an increase in oxygenation time above 20 minutes. After that, the current almost proves to indicate saturation of the solution with

oxygen. Increasing the oxygen concentration leads to increasing the cathodic peak current and decreasing the anodic peak current due to the electrocatalytic reaction of dissolved oxygen and reducing GOD (FAD) (Eq. (13)).

CONCLUSIONS

In this study, CS / GO nanofibers were electrified on the surface of GCE to produce a glucose biosensor. GOx is trapped as an enzyme between two layers of nanofibers. Characteristic analysis showed that a uniform, no-willow morphology with suitable electrochemical properties was obtained when the values of GO and GOx were 2% by weight and 20 mg/mL, respectively. Examination of operating parameters showed that the optimal oxygenation time and pH values are 20 minutes and 7.4, respectively. Electrochemical results showed that the prepared glucose biosensor had high sensitivity (1006.866 μA/mm), wide linear amplitude (0.5-0.20 mmol), and a low detection limit (0.02 mmol). The results of the real-sample analysis showed that the prepared biosensor could be a good candidate for detecting blood glucose levels.

Received: Oct. 4, 2021 ; Accepted: Jan. 31, 2022

References

[1] Al-Jawadi E., Pöller S., Haddad R., Schuhmann W., NADH Oxidation using Modified Electrodes based on Lactate and Glucose Dehydrogenase Entrapped between an Electrocatalyst Film and Redox Catalyst-Modified Polymers, *Microchimica Act*, **177(3-4):** 405–410 (2012).

[2] Wang B., Anzai J.-i., Recent Progress in Lectin-Based Biosensors, *Materials*, **8:** 8590–8607 (2015).

[3] Whiting D.R., Guariguata L., Weil C., Shaw J., IDF Diabetes Atlas: Global Estimates of the Prevalence of Diabetes for 2011 and 2030, Diabetes Res, *Clin. Pract*., **94:** 311–321 (2011).

[4] Hoon Baek S., Roh J., Chan Park Y., Woo Kim M., Shi R., Kumar Kailasa S., Jung Park T., Cu-Nanoflower Decorated Gold Nanoparticles-Graphene Oxide Nanofiber as Electrochemical Biosensor for Glucose Detection, *Materials Science and Engineering: C*, **107:** 110273 (2020).

[5] Azzouz A., Kumar Kailasa S., Kumar P., Ballesteros E., Kim Ki H., Advances in Functional Nanomaterial-based Electrochemical Techniques for Screening of Endocrine Disrupting Chemicals in Various Sample Matrices, *TrAC Trends in Analytical Chemistry*, **113:** 256-279 (2019).

[6] Ferri S., Kojima K., Sode K., Review of Glucose Oxidases and Glucose Dehydrogenases: A Bird's Eye View of Glucose Sensing Enzymes, *J. Diabetes Sci. Technol.*, **5:** 1068 (2011).

[7] Huang K., Wang L., Li J., Gan T., Liu Y., Glassy Carbon Electrode Modified with Glucose Oxidase–Graphene–Nano-Copper Composite Film for Glucose Sensing, *Measurement*, **46:** 378–383 (2013).

[8] Dakshayini B.S., Raghava Reddy K., Mishra A., Shetti N.P., Malode S.J., Basu S., Naveen S., Raghu A.V., Role of Conducting Polymer and Metal Oxide-Based Hybrids for Applications in Ampereometric Sensors and Biosensors, *Microchemical Journal*, **147:** 7-24 (2019).

[9] Kumar S., Bukkitgar S.D., Singh S., Vanshika Singh P., Raghava Reddy K., Shetti N.P., Reddy C.V., Sadhu V., Naveen S., Electrochemical Sensors and Biosensors Based on Graphene Functionalized with Metal Oxide Nanostructures for Healthcare Applications, *Chemistry Europe*, **4:** 5322-5337 (2019).

[10] Buk V., Emregul E., Cebesoy Emregul K., Alginate Copper Oxide Nano-Biocomposite as a Novel Material for Amperometric Glucose Biosensing, *Materials Science and Engineering: C*, **74:** 307-314 (2017).

[11] Muncinelli Caldas E., Novatzky D., Deon M., Weber de Menezes E., Francisco Hertz P., Maria Haas Costa T., Ticona Arenas L., Valmir Benvenutti E., Pore Size Effect in the Amount of Immobilized Enzyme for Manufacturing Carbon Ceramic Biosensor, *Microporous and Mesoporous Materials*, **247:** 95-102 (2017).

[12] Moozarm Nia P., Pei Meng W., Lorestani F., Mahmoudian M.R., Alias Y., Electrodeposition of Copper Oxide/Polypyrrole/Reduced Graphene Oxide as a Nonenzymatic Glucose Biosensor, *Sensors and Actuators B: Chemical*, 2015, 209, 100-108.

[13] Baghayeri M, Glucose Sensing by a Glassy Carbon Electrode Modified with Glucose Oxidase and a Magnetic Polymeric Nanocomposite, *Royal Society of Chemistry Advances*, **5:** 18267-18274 (2015).

[14] Goud K.Y., Kumar Kailasa S., Kumard V., Fai Tsang Y., Lee S.E., Gobi K.V., Kim K-H., Progress on Nanostructured Electrochemical Sensors and their Recognition Elements for Detection of Mycotoxins: A Review, *Biosensors and Bioelectronics*, **121:** 205-222 (2018).

[15] Mao H.Y., Lu Y.H., Lin J.D., Zhong S., Wee A.T.S., Chen W., Manipulating the Electronic and Chemical Properties of Graphene *via* Molecular Functionalization, *Progress in Surface Science*, **88:** 132–159 (2013).

[16] Shetti N.P., Malode S.J., Nayak D.S., Bagihalli G.B., Raghava Reddy K., Ravindranadh K., Reddy C.V., A Novel Biosensor based on Graphene Oxide-Nanoclay Hybrid Electrode for the Detection of Theophylline for Healthcare Applications, *Microchemical Journal*, **149:** 103985 (2019).

[17] Masoudi Farid M., Goudini L., Piria F., Zamani A., Saadati F., Molecular Imprinting Method for Fabricating Novel Glucose Sensor: Polyvinyl Acetate Electrode Reinforced by MnO_2/CuO Loaded on Graphene Oxide Nanoparticles, *Food Chemistry*, **194:** 61-67 (2016).

[18] Li X., Wang X., Zhang L., Lee S., Dai H., Chemically Derived., Ultrasmooth Graphene Nanoribbon Semiconductors, *Science*, **319:** 1229–1232 (2008).

[19] Chang H.X., Tang L.H., Wang Y., Jiang J.H., Li J.H., Graphene Fluorescence Resonance Energy Transfer Aptasensor for the Thrombin Detection, *Anal. Chem.*, **82:** 2341–2346 (2010).

[20] Shan C, Yang H, Song J, Han D, Ivaska A, Niu L, Direct Electrochemistry of Glucose Oxidase and Biosensing for Glucose Based on Graphene, *Anal. Chem.*, **81(6):** 2378-2382 (2009).

[21] Choi J.H., Kim K.J., Kim B.S., Lee H.G., Kim S.H, Covalent Functionalization of Epitaxial Graphene by Azidotrimethylsilane, *J. Phys. Chem. C*, **113:** 9433–9435 (2009).

[22] Zeng Q., Cheng J.-S., Liu X-F.., Bai H.-T, Jiang J-.H., Palladium Nanoparticle/Chitosan-Grafted Graphene Nanocomposites for Construction of a Glucose Biosensor, *Biosensors and Bioelectronics*, **26:** 3456-3463 (2011).

[23] Wang Y., Li Y., Tang L., Lu J., Li J., Application of Graphene-Modified Electrode for Selective Detection of Dopamine, *Electrochemistry Communications*, **11:** 889-892 (2009).

[24] Kang X., Wang J., Wu H., Aksay I.A., Liu J., Lin Y., Glucose Oxidase–Graphene–Chitosan Modified Electrode for Direct Electrochemistry and Glucose Sensing, *Biosensors and Bioelectronics*, **25:** 901-905 (2009).

[25] Almasian A., Olya M.E., Mahmoodi N.M, Preparation and Adsorption Behavior of Diethylenetriamine/Polyacrylonitrile Composite Nanofibers for a Direct Dye Removal, *Fibers and Polymers*, **16:** 1925–1934 (2015).

[26] Han D., Yan L., Chen W., Li W., Preparation of Chitosan/Graphene Oxide Composite Film with Enhanced Mechanical Strength in the Wet State, *Carbohydrate Polymers*, **83:** 653-658 (2011).

[27] Yarandpour M.R., Rashidi A., Khajavi R., Eslahi N., Yazdanshenas M.E., Preparation of Polyacrylic Acid (PAA) / Dextran Nanofibres Modified with Aniline to the Removal of Metal (Pb) from Aqueous Solutions, *Journal of Color Science and Technology*, **4:** 255-271 (2021).

[28] Almasian A., Mahmoodi N.M., Olya M.E., Synthesis of Polyacrylonitrile/Polyamidoamine Composite Nanofibers using Electrospinning Technique and their Dye Removal Capacity, *Journal of the Taiwan Institute of Chemical Engineers*, **49:** 119-128 (2015).

[29] Chiu C.-W., Lin C.-A., Hong P.-D., Melt-Spinning and Thermal Stability Behavior of TiO_2 Nanoparticle/Polypropylene Nanocomposite Fibers, *Journal of Polymer Research*, **18:** 367–372 (2011).

[30] Stankovich S., Dikin D.A., Dommett G.H.B., Kohlhaas K.M., Zimney E.J., Stach E.A., Piner R.D., Nguyen S.T., Ruoff R.S., Graphene-based Composite Materials, *Nature*, **442:** 282–286 (2006).

[31] Shahzad A., Miran W., Rasool K., Nawaz M., Jang J., S.-R. Lim., Sung Lee D., Heavy Metals Removal by EDTA-Functionalized Chitosan Graphene Oxide Nanocomposites, *Royal Society of Chemistry Advances*, **7:** 9764-9771 (2017).

[32] Huang Z., Li Z., Zheng L., Zhou L., Chai Z., Wang X., Shia W., Interaction Mechanism of Uranium(VI) with Three-Dimensional Graphene Oxide-Chitosan Composite: Insights from Batch Experiments, IR, XPS, and EXAFS Spectroscopy, *Chemical Engineering Journal*, **328:** 1066-1074 (2017).

[33] Almasiana A., Olya M.E., Mahmoodi N.M., Zarinabadi E., Grafting of Polyamidoamine Dendrimer on Polyacrylonitrile Nanofiber Surface: Synthesis and Optimization of Anionic Dye Removal Process by Response Surface Methodology Method, *Des. Wat. Treat.*, **147:** 343-363 (2019).

[34] Datsyuk V., Kalyva M., Papagelis K., Parthenios J., Tasis D., Siokou A., Kallitsis I., Galiotis C., Chemical Oxidation of Multiwalled Carbon Nanotubes, *Carbon*, **46:** 833–840 (2008).

[35] Li Z., Sheng L., Meng A., Xie C., Zhao K., A Glassy Carbon Electrode Modified with a Composite Consisting of Reduced Graphene Oxide, Zinc Oxide and Silver Nanoparticles in a Chitosan Matrix for Studying the Direct Electron Transfer of Glucose Oxidase and for Enzymatic Sensing of Glucose, *Microchimica Acta*, **183:** 1625–1632 (2016).

[36] Men Z., Fang W., Li D., Li Z., Sun C., Raman Spectra from Symmetric Hydrogen Bonds in Water by High-Intensity Laser-Induced Breakdown, *Sci. Rep.*, **4:** 4606 (2014).

[37] Rafiei S., Optimization and Production of Polyacrylonitrile based Activated Carbon Nanofibers for Dye Wastewater Treatment, *J. Co. Sci. Tech.*, **14(4):** 281-294 (2020).

[38] Berenjian A., Maleknia L., Chizari Fard G.h., Almasian A., Mesoporous Carboxylated Mn_2O_3 Nanofibers: Synthesis, Characterization and Dye Removal Property, *J. Ta. Inst. Ch. En.*, **86:** 57-72 (2018).

[39] Almasian A, Olya M. E, Mahmoodi N. M, Synthesis of Polyacrylonitrile/Polyamidoamine Composite Nanofibers Using Electrospinning Technique and Their Dye Removal Capacity, *J. Ta. Inst. Ch. En.*, **49:** 119-128 (2015).

[40] Shekarabi A., Monajjemi M., Experimental & Theoretical investigation of Glucose – Graphene Hybrid for increasing the Natural Gas Storage, *Iran. Chem. Chem. Eng. (IJCCE)*, **41(2):** 392-388 (2022).

[41] Wang J., Electrochemical Glucose Biosensors, *Chem. Rev.*, **108:** 814–825 (2008).

[42] Foroughi F., Rahsepar M., Hadianfard M.J., Kim H., Facile Synthesis and Electrochemical Performance of Graphene-Modified Cu_2O Nanocomposite for Use in Enzyme-Free Glucose Biosensor, *Iranian Journal of Chemistry and Chemical Engineering (IJCCE)*, **39(2):** 1-10 (2020).

[43] Haghighi B., Tabrizi M.A., Direct Electron Transfer from Glucose Oxidase Immobilized on an Overoxidized Polypyrrole Film Decorated with Au Nanoparticles, *Colloids Surf. B*, **103:** 566-571 (2013).

[44] Chen L., Xie H., Li J., Electrochemical Glucose Biosensor based on Silver Nanoparticles/Multiwalled Carbon Nanotubes Modified Electrode, *J. Solid State Electrochem*, **16:** 3323-3329 (2012).

[45] Kang X., Wang J., Wua H., Aksay I.A., Liu J., Lin Y., Glucose Oxidase–Graphene–Chitosan Modified Electrode for Direct Electrochemistry and Glucose Sensing, *Bio. Bio.*, **25:** 901-905 (2009).

[46] Wang Y., Li Y., Tang L., Lu J., Li J., Application of Graphene-Modified Electrode for Selective Detection of Dopamine, *Electrochemistry Communications*, **11(4):** 889-892 (2009).

[47] Fang L., Liu B., Liu L., Li Y., Huang K., Zhang Q., Direct Electrochemistry of Glucose Oxidase Immobilized on Au Nanoparticles-Functionalized 3D Hierarchically ZnO Nanostructures and its Application to Bioelectrochemical Glucose Sensor, *Sensors and Actuators B: Chemical*, **222:** 1096-1102 (2016).

[48] Zai M., Makshoof Athar M., Electrochemical Evaluation of Phanerocheaete Chrysosporium Based Carbon Paste Electrode with Potassium Ferricyanide Redox System, *Int. J. Electrochem. Sci.*, **10:** 6690 – 6702 (2015).

[49] Wen D, Liu Y, Yang G.C, Dong S.J, Electrochemistry of glucose oxidase immobilized on the carbon nanotube wrapped by polyelectrolyte, *Electrochim. Acta*, **52**, 5312–5317 (2007).

[50] Almasian A., Najafi F., Maleknia L., Giahi M., Mesoporous MgO/PPG Hybrid Nanofibers: Synthesis, Optimization, Characterization and Heavy Metal Removal Property, *New J. Chem.*, **42:** 2013-2029 (2018).

[51] Zeng Q., Cheng J.-S., Liu X.-F., Bai H.-T., Jiang J.-H., Palladium Nanoparticle/Chitosan-Grafted Graphene Nanocomposites for Construction of a Glucose Biosensor, *Biosensors and Bioelectronics*, **26:** 3456-3463 (2011).

[52] Liu Q., Lu X.B., Li J., Yao X., Li J.H., Direct Electrochemistry of Glucose Oxidase and Electrochemical Biosensing of Glucose on Quantum Dots/Carbon Nanotubes Electrodes, *Biosensors and Bioelectronics*, **22:** 3203 (2007).

[53] Al-Aibi S.M., Balassim Mahood H., Derwish G.h., Obaid Sharif A., Separation Efficiency of Glucose and Maltose from Industrial Effluent by Granular Activated Carbon, *Iranian Journal of Chemistry and Chemical Engineering (IJCCE)*, **37(6):** 95-105 (2018).

[54] KHatibi A., Heydari M., Zarrabi M., The Effect of Formetanate Hydrochloride on the Glycated Human Hemoglobin, *Iranian Journal of Chemistry and Chemical Engineering (IJCCE)*, **41(5):** 1804-1811 (2022).